Does Microwave Exposure at Different Doses in the Pre/Postnatal Period Affect Growing Rat Bone Development?

Aysegul Akar KARADAYI[1], Hayrunnisa Yeşil SARSMAZ[2], Ayşe ÇİĞEL[3], Begüm Korunur ENGİZ[4], Nilüfer Akgün ÜNAL[1], Sebati Sinan ÜRKMEZ[5], Seren Gülşen GÜRGEN[6]

[1]Department of Biophysics, Faculty of Medicine, Ondokuz Mayis University Samsun, Republic of Türkiye, [2]Department of Histology and Embryology, Manisa Celal Bayar University, Manisa, Republic of Türkiye, [3]Department of Physiology, Faculty of Medicine, Izmir Democracy University, Izmir, Republic of Türkiye, [4]Department of Electrical and Electronical Engineering, Faculty of Engineering, Ondokuz Mayıs University, Samsun, Republic of Türkiye, [5]Department of Medical Biochemistry, Faculty of Medicine, Ondokuz Mayis University, Samsun, Republic of Türkiye, [6]Department of Histology and Embryology, School of Vocational Health Service, Manisa Celal Bayar University, Manisa, Republic of Türkiye

Received June 1, 2023
Accepted January 15, 2024

Summary

Effects of pre/postnatal 2.45 GHz continuous wave (CW), Wireless-Fidelity (Wi-Fi) Microwave (MW) irradiation on bone have yet to be well defined. The present study used biochemical and histological methods to investigate effects on bone formation and resorption in the serum and the tibia bone tissues of growing rats exposed to MW irradiation during the pre/postnatal period. Six groups were created: one control group and five experimental groups subjected to low-level different electromagnetic fields (EMF) of growing male rats born from pregnant rats. During the experiment, the bodies of all five groups were exposed to 2.45 GHz CW-MW for one hour/day. EMF exposure started after fertilization in the experimental group. When the growing male rats were 45 days old in the postnatal period, the control and five experimental groups' growing male and maternal rats were sacrificed, and their tibia tissues were removed. Maternal rats were not included in the study. No differences were observed between the control and five experimental groups in Receptor Activator Nuclear factor-kB (RANK) biochemical results. In contrast, there was a statistically significant increase in soluble Receptor Activator of Nuclear factor-kB Ligand (sRANKL) and Osteoprotegerin (OPG) for 10 V/m and 15 V/m EMF values. Histologically, changes in the same groups supported biochemical results. These results indicate that pre/postnatal exposure to 2.45 GHz EMF at 10 and 15 V/m potentially affects bone development.

Key words

Microwave • Bone cell • RANK • sRANKL • OPG

Corresponding author

A. A. Karadayi, Department of Biophysics, Medicine Faculty, Ondokuz Mayıs University, Samsun, Republic of Türkiye. E-mail: aysegula@omu.edu.tr

Introduction

Wireless-Fidelity (Wi-Fi) devices at 2.45 GHz Microwave (MW) frequency used for communication purposes contain low-power Radio frequency (RF)-Electromagnetic Field (EMF) transceivers that support wireless local area networks (WLANs). Additionally, Wi-Fi has less severity than standard Specific absorption rate (SAR) limit values for RF or MW given by the International Commission on Non-Ionizing Radiation Protection ICNIRP 2020 report [1]. As it is known, the excess fluid content of pregnant women's amino fluids and growing children's total fluid content are higher than that of adults. Moreover, the interaction of EMF with water molecules increases the exposure, but they are not considered to be within the limit values. Considering that the EMF interaction with water molecules may create a thermal or non-thermal effect at very low-level EMF

exposures, these adverse effects may increase for pregnant women and their offspring, especially for bone mechanisms. Mechanisms studies related to the head, torso and/or other organs at low/high level EMF that is low/high Specific Absorbed Rate (SAR) exposure, the research results for these local areas are also extensively covered in reviews and the ICNIRP 2020 report [1-3]. However, although there are a lot of research and studies on the positive and negative effects of low frequencies on limbs and bone mechanisms in the reports [1,4-8], there is very little research on bone at RF and MW frequency and especially at low-level EMF exposure during pre/postnatal period [9].

Bones are dynamic tissues in which bone resorption and formation are continuously repeated in a homeostatic mechanism of "coupling" between these processes [10]. Because of coupling and absorption into the body of MW [1], bone development during ossification in the prenatal period might be affected by environmental or physical exposures such as MW irradiation. Osteoclasts are cells of hematopoietic origin. Osteoclastic bone resorption is indispensable in remodelling or replacing bone during bone development (modelling) and growth (remodelling). Due to any external factor, such as bone fracture, injury, or exposure to toxicity or devices, a high amount of osteoclast activity causes increased bone resorption and osteopenia. At the same time, reduced activity leads to an imbalance in remodelling in favor of osteopetrosis [11]. Recently, osteocytes have been recognized as essential choreographers of skeletal homeostasis. [12]. Importantly, osteocyte apoptosis or dysregulation has been implicated in several diseases, including osteoporosis, osteoarthritis, osteomalacia, and others [13]. Recent studies also showed that hypertrophic chondrocytes and osteocytes are a significant source of the Receptor Activator nuclear factor-kB Ligand (RANKL) during mineralized cartilage resorption and adult bone remodelling [14]. It has been proposed that the soluble forms of RANKL are Receptor Activator of Nuclear factor-kB Ligand (sRANKL). The sRANKL has more potent activity and essential roles in osteolysis induced by tumors. The sRANKL derives from the membrane form due to either proteolytic cleavage or alternative splicing [15]. The binding of the RANKL to the RANK prolongs osteoclast survival by suppressing apoptosis [16]. The effect of the RANKL is blocked by osteoprotegerin (OPG), a glycoprotein secreted by osteoblasts that acts as a decoy receptor for the RANKL [17]. The term OPG has been coined for its effects of protecting against bone loss [18]. The balance between the RANKL and the OPG is regulated by cytokines and hormones, determining osteoclast functions. The RANKL/OPG ratio alteration is critical in bone pathogenesis and increases bone resorption [19,20]. The Receptor Activator Nuclear factor-kB (RANK) is expressed on the surface of osteoclast progenitors and mature osteoclasts [21]. Osteoblasts, osteocytes, and bone marrow stromal cells primarily secrete the RANKL. The binding between the RANK and, specifically, the RANKL causes osteoclast genesis and bone resorption. Thus, the OPG, a decoy receptor for the RANKL secreted by osteoblasts to inhibit osteoclast formation by antagonising RANK/RANKL signalling, is a target for treating bone loss-related diseases such as osteoporosis [22,23]. Most studies on bone metabolism have focused on the effects of EMF on the RANK/RANKL/OPG pathway required for osteoclast genesis and bone resorption of osteoclasts [4,24].

Considering the literature review, we aimed to investigate the effects of 2.45 GHz MW radiation at different EMF values on bone in growing rats by supporting it with biochemical and histological parameters. Our study is the first in the literature focusing on the thermal/non-thermal effect level of 2.45 GHz MW exposure on the bone at different low-level EMF values.

Materials and Methods

Experimental groups

This study used growing Wistar rats randomly generated from 12 mother rats with two each and six experimental groups with different EMF values. This study protocol was approved by the Ondokuz Mayis University Animal Experiments Theoretical Ethics Committee (OMÜ HAYDEK) with decision number 2019/23. Maternal and growing rats were kept in a 12-hour day/night cycle at room temperature of 22-25 °C and humidity of 40-50 % by the circadian rhythm. They were given food and water *ad libitum* for the entire study period, except for the exposure time. In the study, each group was exposed to 2.45 GHz MW frequency at different EMF values, except for the control group. The experimental growing rats were exposed to MW for 66 days from pregnancy. The groups were randomly formed as six groups of maternal rats before pregnancy, and growing rats belonging to the groups of maternal rats were used. Group I (G1) (n=9): growing

rats in this group were constituted as the control group and were fed with standard rat chow during growing. The control group rats had not been exposed to any EMF. Other groups were group II (G2, n=8, exposed to 0.6 V/m EMF), group III (G3, exposed to 1.9 V/m EMF, n=8), group IV (G4, exposed to 5 V/m EMF, n=8), group V (G5, exposed to 10 V/m EMF, n=8), group VI (G6, exposed to 15 V/m EMF, n=8), respectively. MW radiation was applied from the zeroth day of pregnancy to the growing rat period (66 days in total).

Exposure design, thermal, and EMF measurements

Exposure system and experimental design: 2004X-RF Wi-Fi system generator with a Monopole antenna and 0-1 Watt maximum out power (2004X-RF Wi-Fi system generator, Everest Co., Adapazari, Turkey) was used to generate MW radiation at a frequency of 2.45 GHz MW in this study. MW radiation exposure of the rats was in the 12-slice pie-cage restrained, and the antenna was placed in the middle of the 12-slice pie-cage restrained to ensure equal electric field distribution. Before the study, the electric field levels in the experimental environment were determined using an electric field meter (Narda EMR-300 broadband, Narda-Safety Test Solutions, Germany) with the isotropic electric field strength probe (EMR300 Probe model, Type 8C. 2244/90.21, Germany), while band selective electric field strength levels were determined (Narda SRM-3006, Narda-Safety Test Solutions, Germany). The highest EMF strength value was 92 mV/m with Narda EMR-300 and 103 mV/m with Narda SRM-3006. Magnetic Field (MF) strength levels were measured using a low-frequency signal analyzer (Spectra NF-5035, AARONIA AG, Germany), and the repetition time and frequency were monitored using a spectrum analyser (RF-Explorer 6G Combo, EMRSS, Germany). The highest MF strength level in the environment is 286 μA/m, while the highest value in the 2.45 GHz MW signal measurements taken with the RF-Explorer 6G Combo is -70 dBm. Thermal and EMF measurements: after the experimental electric and magnetic field measurements, the temperature images of growing rats before and after exposure were recorded with a TESTO brand 870-02 model thermal camera to make thermal evaluations at different EMF values. By taking the average temperature values of the body regions taken from the thermal images of 10 different days for each group, the average temperature values of the body region were calculated as between 31.10±0.04 °C and 31.21±0.05 °C for group 1, between 31.05±0.04 °C and 31.37±0.06 °C for group 2, between 31.16±0.04 °C and 31.66±0.07 °C for group 3, between 31.14±0.04 °C and 31.90±0.08 °C for group 4, between 31.07±0.05 °C and 32.16±0.11 °C for group 5, between 31.17±0.05 °C and 32.51±0.13 °C for group 6. For the head and body regions, the mean temperature changed in all groups before and after exposure (The mean variation was between 0.2 and 1.37 °C and 0.1 to 1.33 °C) in both regions, head and body regions, groups 5 and 6. While it was above 1 °C, the average temperature change in the other groups was less than 1 degree. To calculate the SAR values of growing rats subjected, the means of EMF values measured for 66 days of growing rats subjected to MW radiation were 0.65±0.11, 1.95±0.25, 4.97±0.32, 10.26±0.52, and 15.40±0.60 V/m for Groups 2, 3, 4, 5, 6, respectively.

SAR calculation, electric field strength, and SAR distributions

To determine the effect of the applied MW radiation level in SAR values, the experiment environment was created using an electromagnetic simulation software (Computer Simulation Technology, CST Studio Suite, version of 2018, USA) program, which helps the discretization of Maxwell equations by Finite Integration Technique (FIT), and performing numerical simulation. For this purpose, a monopole antenna operating at 2.45 GHz was created and placed at the center of the modelled Plexiglas holder as in the laboratory. To simulate the experiment and calculate SAR distribution over rats, 12 computational "Rat" models were placed in the Plexiglas holder. The SAR (10g) values were calculated from EMF values (0.65±0.11, 1.95±0.25, 4.97±0.32, 10.26±0.52, and 15.40±0.60 V/m) measured for exposed groups according to the International Electrotechnical Commission (IEC) and Institute of Electrical and Electronics Engineers (IEEE), IEC/IEEE 62704–1 standard. The peak SAR 10g values over the bone tissues for different doses of EMF were obtained and given in Figure 1B, C, D, E, and F. The figures show that the peak SAR 10g values are 0.46 μW/kg, 0.51 mW/kg, 3.32 mW/kg, 14.4 mW/kg, and 33.8 mW/kg for the given exposure levels, respectively.

Biochemical Assays

ELISA Test

The RANK (Biotechnology, BTLab E0288Ra rat ELISA kit, Chine), the sRANKL (Fine test ER1604

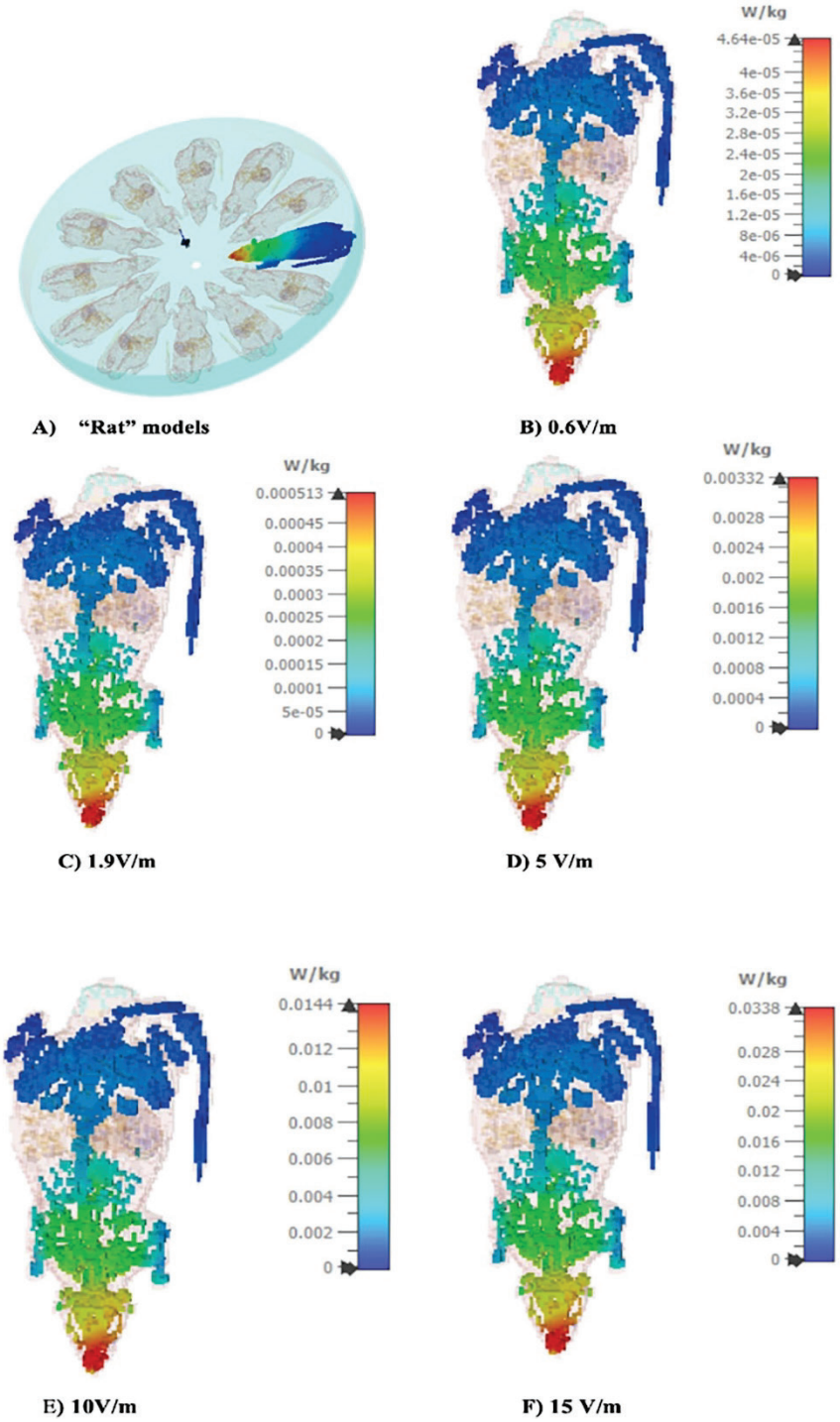

Fig. 1. Rat model simulation and SAR 10g distribution on the bone tissue of the following: (**A**) Rat model, (**B**) 0.6 V/m, (**C**) 1.9 V/m, (**D**) 5 V/m, (**E**) 10 V/m, (**F**) 15 V/m.

Rat, Chine), and the OPG (Fine test, ER1212 Rat, Chine) levels in serum were evaluated with enzyme-linked immunosorbent assay (ELISA) kits by the kit procedure. Absorbance was measured at 450 nm wavelength with Synergy HT, Multi-Detection Microplate Reader, and BIO-TEK plate reader device (Biotek elx800, Germany). Results were given as ng/ml for RANK and pg/ml for sRANKL and OPG protein.

Histological Evaluation

Hematoxylin-eosin stain method

The removed tibia was fixed in 10 % neutral formalin for 24 h. They were then decalcified in a formic acid solution for four days. Following the histological tissue follow-up procedures, 5-micron serial sections were applied to the bone sections taken from the tibia diaphysis lines, and Hematoxylin-eosin stain (HHS32,

Merck, Darmstadt, Germany) was used to some sections. The obtained preparations were examined and photographed under a research microscope (Olympus CX31RTSF, Tokyo, Japan), and compact bone thickness measurements were made on digital images transferred to a computer using the ToupTek XCamView Image Processing and ToupTek analysis software application (ToupTek Microsystem, No: V3.0-20180809, China). Five random slides were selected from serial sections taken from each tissue, and compact bone thickness was measured with the ToupTek analysis system at ×400 magnification in 10 different areas on each slide. Counts of osteoblast, osteocyte, and osteoclasts were made in photographs taken on the same slides and from the same regions at ×400 magnification in 10 different areas.

Immunohistochemical method

Some of the serial sections taken were reserved for immunohistochemistry staining. The sections incubated at 60 °C for one night were deparaffinized in xylene and dehydrated in decreasing alcohol series and then were boiled for antigen retrieval in citrate buffer (10 mM, pH 6.0) in a microwave for 15 min. They were incubated to inhibit endogenous peroxidase activity with hydrogen peroxidase (TA-125-HP, Thermo Fisher Scientific, CA, USA) for 15 min. The sections were incubated in blocking serum (Ultra V Block, TP-060-HL; NeoMarker, Fremont, CA, USA) for 10 min and incubation processing was continued with primary antibodies caspase-3 (SC-56053, Santa Cruz Biotechnology, CA, USA) and caspase 9 (RB-1205-PO, Santacruz Biotechnology, CA, USA) for 60 min at room temperature and in a humid environment. The antigen-antibody complex (HRP, TP-125-HL, Thermo Fisher Scientific, CA, USA) was detected with biotinylated secondary antibody and streptavidin-peroxidase complex (20 min), and labelling was performed using AEC (3-Amino-9-Ethylcarbazole, TA-060-HA, Labvision, CA, USA). Mayer's hematoxylin (TA-125-MH, Thermo Fisher Scientific, USA) was used as a floor paint. The stained glasses were covered with a coverslip with an ultra-mount, examined with an Olympus CX31 microscope (Olympus CX31RTSF, Tokyo, Japan), photographed and counted using the ToupTek analysis system (ToupTek Microsystem, No: V3.0-20180809, China). In the staining, ten areas were selected randomly at ×400 magnification in each preparation, and the H-score was calculated according to the density of positive cell uptakes stained in the tissues and the percentage of uptake.

TUNEL staining

An *in situ* apoptosis detection (TUNEL) kit (S7101, Millipore, Darmstadt, Germany) was used to detect DNA fragmentation and apoptotic cell death. The preparations, maintained at 60 °C for one hour to facilitate deparaffinization, were kept in xylol twice for 15 min to complete the deparaffinization. Then, the sections, which were passed through the ethanol series, were incubated with 20 µg/ml proteinase K (107393, Merck, Darmstadt, Germany) for 10 min after they were passed through distilled water twice for 5 min to purify them from alcohol. After washing with PBS (AM9625, Phosphate Buffered Saline, Thermo Fisher Scientific, CA, USA), endogenous peroxidase activity was blocked in tissues that were left active with 3 % hydrogen peroxide (TA-125-HP, Thermo Fisher Scientific, CA, USA) for 15 min. Sections washed with PBS were incubated in a balanced buffer for 10-15 min and in a humid environment at 37 °C for 60 min in TdT enzyme (S7101, Millipore, Darmstadt, Germany) (77 µl Reaction Buffer + 33 µl TdT Enzyme). It was then incubated for 10 min in a pre-warmed stop/wash buffer at room temperature and incubated in Anti-Digoxigenin (S7101, Millipore, Darmstadt, Germany) for 45 min. Careful washing with PBS was performed at each step. After washing, DAB staining (S7101, Millipore, Darmstadt, Germany) was performed to identify TUNEL-positive cells. Methyl green (M8884, Merck, Darmstadt, Germany) was applied for 5 min. For the floor painting, after the stained slides were dehydrated by passing through increasing alcohol series, they were kept in xylol for 20 min to transparency. Then, the entella and coverslip were closed, and their photographs were taken under the CX31 light microscope (Olympus CX31RTSF, Tokyo, Japan).

Statistical analysis

Statistical evaluation of biochemical data was performed using the GraphPad Demo program (GraphPad Prism-8, Software version 8, US), and “mean standard deviation (SD)” values were used in the analysis of the data. One-way ANOVA was used to compare the means of the data of the groups in a single direction. In addition, the Tukey *post hoc* test was used to determine the difference between which groups, and differences at the $p<0.05$ level were considered significant. Histological

data, including osteoblast, osteoclast, osteocyte, caspase 3, 9, and Tunel data, were obtained using the GraphPad Prism-8 Demo program. Mean ± Standard Deviation (SD) values were used to analyse the data. One-way ANOVA was used to compare the means of the data belonging to the groups. Tukey's test was used for osteocyte, osteoblast, and osteoclast data, and a *post hoc* test was used for caspase 3, 9, and tunel data to determine which groups the difference was between.

Results

RANK, sRANKL and OPG in serum

In our study, no significant difference was found between the RANK levels of control and other different EMF MW irradiation groups ($p>0.05$, Table 1, Fig. 2A). When the sRANKL levels of the control group and the other groups were compared, a statistically significant difference was found only in Group 5 and Group 6. However, it was lower than the G1 control group in all groups ($p<0.05$, Table 1, Fig. 2B). The sRANKL levels of Group 2, Group 3 and Group 4 were not different from each other ($p>0.05$, Table 1, Fig. 2B). When the G1 (control group) and EMF exposure groups in other groups were compared, there was an increase in OPG levels, but there was a significant difference in OPG levels only in the 10 V/m (G5) and 15 V/m (G6) exposure groups, as in the sRANKL ($p<0.05$). OPG level of G1 was lower than all other groups ($p<0.05$), and OPG levels of G2, G3, and G4 were not different from each other ($p>0.05$, Table 1, Fig. 2C). In our study, the lowest sRANKL/OPG levels and statistically significant difference between the groups were obtained in Groups 4, 5 and 6. The sRANKL/OPG ratio of G6 was lower than all other groups ($p<0.05$ Table 1, Fig. 2D). As a result, in the comparison of the G1 control group and other exposure groups, there was no statistical change in RANK levels. At the same time, there was a significant difference in sRANKL and OPG levels in the G5 (10 V/m) and G6 (15 V/m) groups. However, there was a substantial difference in the sRANKL/OPG level in G4, G5, and G6 compared to the control, and there was a decrease in all groups compared to the control group.

Histological Findings

Hematoxylin-Eosin Findings

According to the hematoxylin-eosin findings, it was observed that the compact bone in the diaphysis region of the tibia preserved its normal and healthy structure in the control group (Fig. 3A1). Osteoblasts, and osteoclasts were in a normal structure and were laid on the inner surface of the bone (Fig. 3A2, A). The Walkman canals in the bone were in normal structure, the bone lamellae around the channels were correctly located, and the osteocytes in the lacunae were in standard structure (Fig. 3, A2). In Groups 2, 3, and 4, the structure of the Haversian canal system of the compact bone was disrupted. Abnormal enlargements in the Walkman canals of the bone were remarkable (Fig. 3 B2, C2, D2). In Groups 5 and 6, severe and unhealthy enlargements in the Walkman and Haversian canals were noted, in which the structure of the compact bone was severely deteriorated (Fig. 3E2, F2).

Tibia compact bone thickness measurement, osteocyte, osteoclast, and osteoblasts findings

Compared to the control group G1, although the thickness of the tibia decreased as the exposure increased, there was no significant difference in thickness in the G2, G3, and G4 groups according to the *post hoc* (Tukey) comparative analysis results in the analysis performed for all groups ($p>0.05$). There was a significant difference in thickness between only the G1 group and the groups G5 and G6, the group with the highest EMF exposure ($p<0.05$) (Fig. 4A). Osteocytes decreased from the G3 group compared to the G1 control group (Fig. 4B). According to the results of *post hoc* (Tukey) comparative analysis, there was a significant difference between all groups in terms of osteoblast counts ($p<0.05$) (Fig. 4D). There was a substantial difference between the G1 and G5 groups and between the G1 and G6 groups in osteoclast counts ($p<0.05$), but there was no significant difference between other groups ($p>0.05$) (Fig. 4C).

Immunohistochemical and TUNEL straining findings

In caspase3 immunostaining, weak reactions were observed in G1 and G2 tibia diaphysis rupture osteoblasts, osteocyte, and Haversian channels in bone tissue. In contrast, moderate expiration was observed in osteoblasts and occasionally in some osteocytes in G3 (Fig. 5A: A1, B1, C1). However, there was no staining in the Haversian canals (Fig. 5A: C1). In G4 and G5, the reaction ranged from moderate to strong in osteoblasts and Haversian canals. The number of caspase3-reactive cells was increased in osteocytes (Fig. 5A: D1, E1). In G6, compelling caspase 3 expression was noted in osteoblasts, osteocytes, and Haversian ducts (Fig. 5A: F1). Caspase 9 immunostaining was weaker overall in the

groups when compared with Caspase 3. Weak reactions were observed in osteoblast, osteocytes, and Haversian channels in and G3 (Fig. 5A: A2, B2). In G3, G4, and G5, a weak to moderate reaction was detected in osteoblast, osteocytes and Haversian channels (Fig. 5A: C2, D2, E2). Strong expression was detected in some osteocytes and Haversian ducts in G6 (Fig. 5A: F2). With the Tunel method, while the cells were almost absent in the compact bone of the tibia diaphysis region in G1 and G2 (Fig. 5B: A, B), the number of cells in osteoblasts and osteocytes increased (Fig. 5B: C, D). It was noted that the number of cells showing reaction in osteoblasts and osteocytes in G5 and especially G6 increased considerably (Fig. 5B: E, F). Compared to the G1 control group, *post hoc* (Tukey) comparative analysis revealed a significant difference between the caspase 3, caspase 9, and Tunel staining groups except for G2 ($p<0.05$) (Table 1).

Table 1. Biochemical analysis and immunohistochemical data. in comparison with G1.

Groups (n=8)	**RANK (ng/ml)**	**sRANKL (pg/ml)**	**OPG (pg/ml)**	**sRANKL/ OPG**	**Caspase 3 (count)**	**Caspase 9 (count)**	**Tunel (count)**
Control							
G1	9.37±0.33	227.76±16.45	118.03±51.56	3.94±0.88	27.00±4.89	23.50±4.24	2.62±1.40
Expose							
G2	9.84±0.24	238.04±14.95	189.19±53.30	2.49±0.85	36.25±4.06	31.75±4.06	3.00±1.85
G3	10.04±0.09	269.99±20.70	217.46±88.01	1.83±0.70	**55.50±7.34***	**47.62±6.09***	**17.00±3.46***
G4	8.85±0.38	242.33±10.69	258.85±14.89	**0.95±0.07****	**100.50±7.34***	**64.50±7.34***	**18.50±2.44***
G5	9.80±0.48	**306.50±9.27***	**380.11±18.37***	**0.83±0.06***	**140.25±10.81***	**97.50±4.81***	**23.50±2.44***
G6	10.35±0.29	**296.80±10.12***	**394.86±10.84***	**0.77±0.03***	**256.25±17.31***	**130.00±9.79***	**34.50±4.03***

All data are given as mean ± SD, SD standard deviation, * represents statistical significance, and ** represents strong significance. * $p<0.05$; ** $p<0.001$; Compared to the G1 control group.

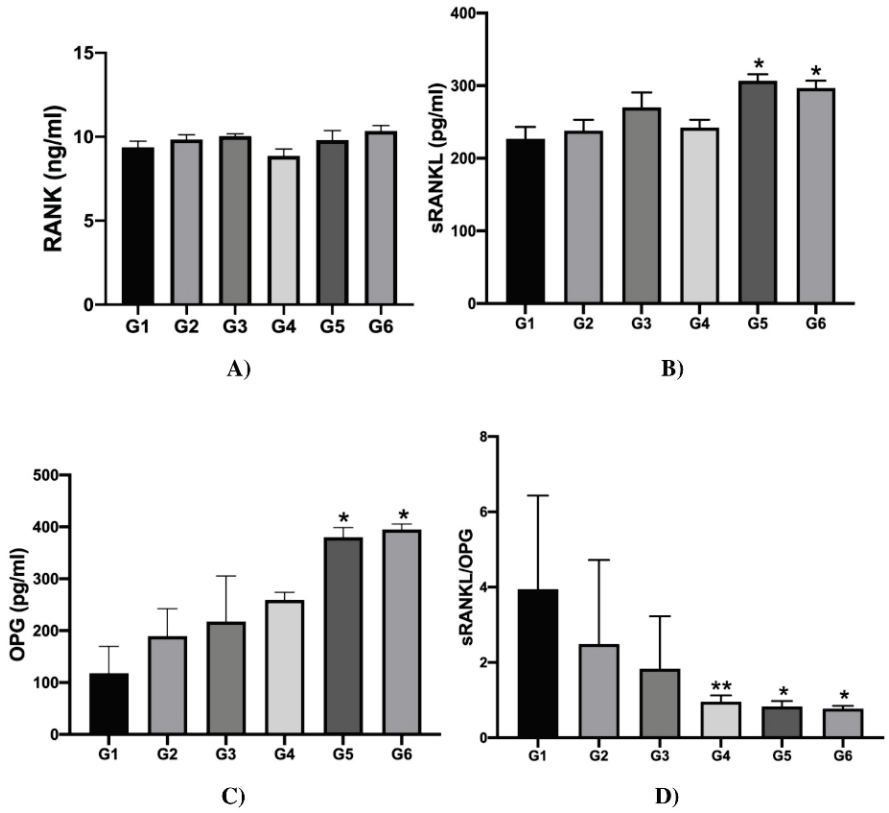

Fig. 2. (**A**) RANK, (**B**) sRANKL, (**C**) OPG levels, and (**D**) sRANKL/OPG ratio. * indicates significance between G1 and G5, G6 groups ($p<0.05$). ** indicates the significance between G1 and G4 groups ($p<0.05$). * $p<0.05$; ** $p<0.01$.

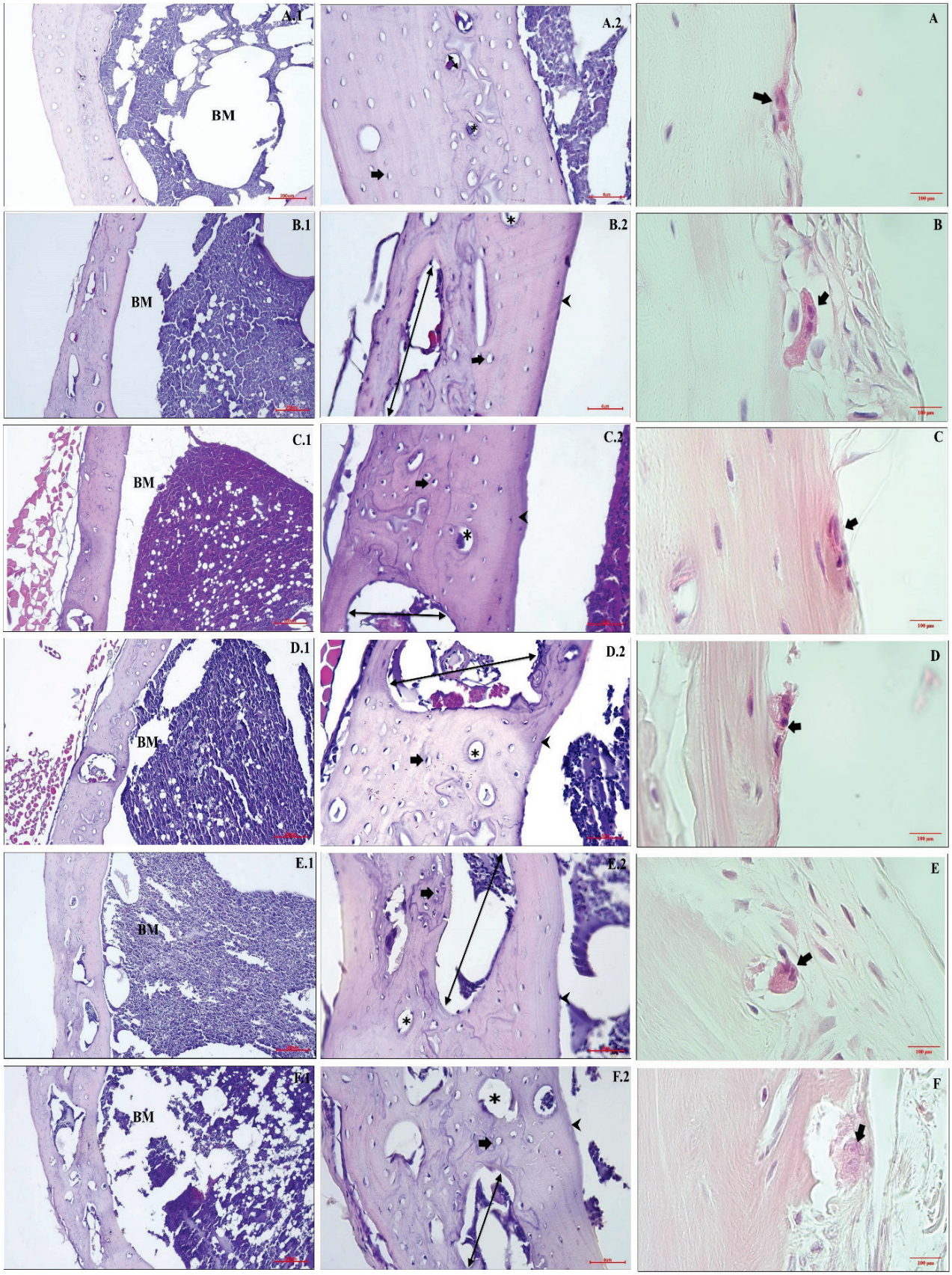

Fig. 3. Hematoxylin-Eosin staining images of tibia diaphyseal compact bone. Control group: Group1 (A1, A2, **A**), Exposed groups: Group2 (B1, B2, **B**), Group3 (C1, C2, **C**), Group4 (D1, D2, **D**), Group5 (E1, E2, **E**), Group6 (F1, F2, **F**). (**A**) BM (1): Bone marrow, ×100, Bar = 200 µm and (2): ➤: Osteoblast, ➡: Osteocyte, ✱: Haversian canals, ↔ : Walkman canals, ×400, Bar = 4 µm; (**B**) Osteoclast (➡) ×1000, Bar = 100 µm.

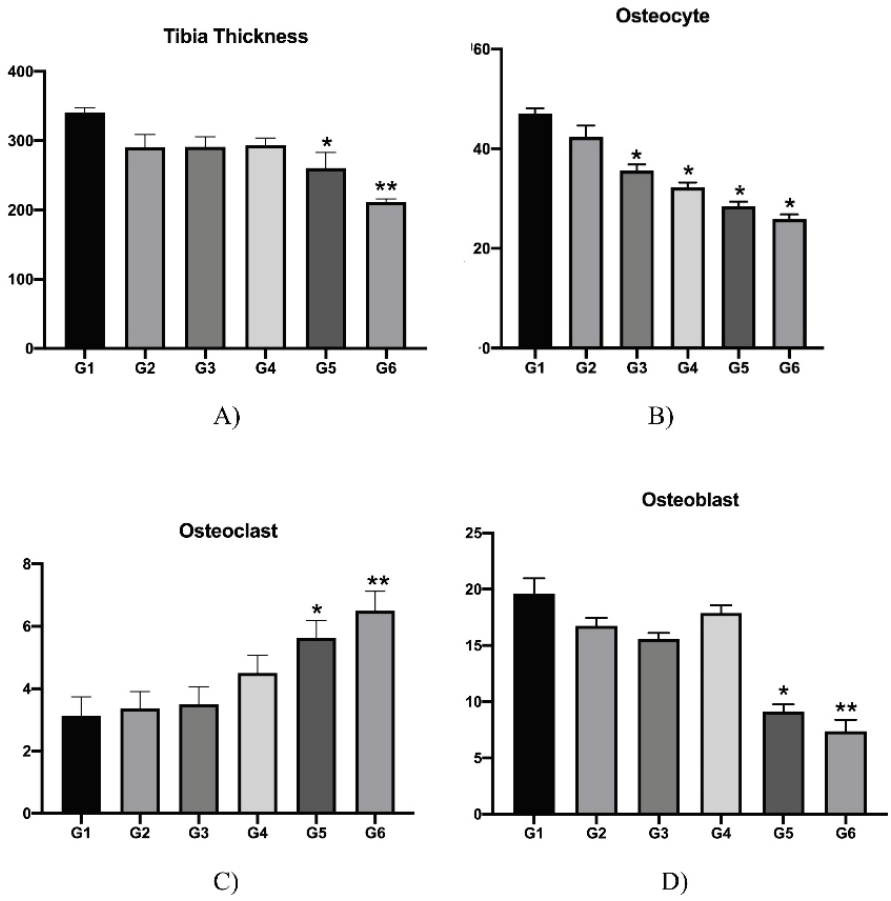

Fig. 4. (**A**) Tibia compact bone thickness (μm) and, (**B**) Osteocyte, (**C**) Osteoclast, and (**D**) Osteoblast counts: Mean ± Standard deviation distributions at between groups. Statistical differences are given in comparison with G1. * G1 and G5, groups; ** indicates the significance between G1 and G6 groups ($p<0.05$). (* $p<0.05$; ** $p<0.01$).

Discussion

In this study, we examined the effects and differences in bone formation between different EMF exposure groups and the control group to investigate the effect of exposure to 2.45 GHz MW radiation on pre/postnatal development. We observed functional and histomorphological changes associated with bone formation on the bone with 10 and 15 V/m EMF exposure in growing rats exposed to MW radiation. As far as we know, there are very few studies on the effects of EMF on bone and the level of thermal and non-thermal effects in developing rats, in line with RANK, sRANKL, OPG, RANKL/OPG, and histological findings are available. In this experimental model, while we observed a statistically significant increase in biochemical, sRANKL, and OPG values in the G5 and G6 groups where thermal temperature increases exceeded 1 °C in thermal measurements, we observed a decrease in the sRANKL/OPG ratio in these groups. Because of the statistical evaluations of histological data, we observed a statistical reduction in tibia thickness, osteoblast, and osteocyte numbers in the G5 and G6 groups, especially. In contrast, an increase in the number of osteoclasts and caspase 3, 9 Tunel evaluations were observed. At the same time, there was no change in the RANK level.

Bone remodelling begins early in skeletal development. The new bone formation is the task of osteoblasts, whereas bone resorption is the task of osteoclasts. Both processes are controlled by osteocytes [25]. Bone homeostasis depends on strictly balanced activities between bone formation by osteoblasts and bone resorption by osteoclasts. However, RANKL/OPG signalling is a complex that regulates bone remodelling. RANKL functions as a master regulator of osteoclast differentiation and function, while OPG is an inhibitor of bone resorption. An imbalance of bone formation and resorption can cause various bone diseases. Various stress factors, such as MW irradiation, can affect bone formation and resorption, especially during development. It has been proven by many studies that ionising radiation negatively affects bone metabolism in adults [26]. The effects of low and high-frequency non-ionizing radiation on bone metabolism are still a matter of debate, and it is being investigated at which frequencies they have positive or adverse effects. The EMF can inhibit osteoclast formation by affecting the RANK/RANKL pathway. In a study conducted with ovariectomized (OVX) rats, the low-frequency pulsed EMF inhibited

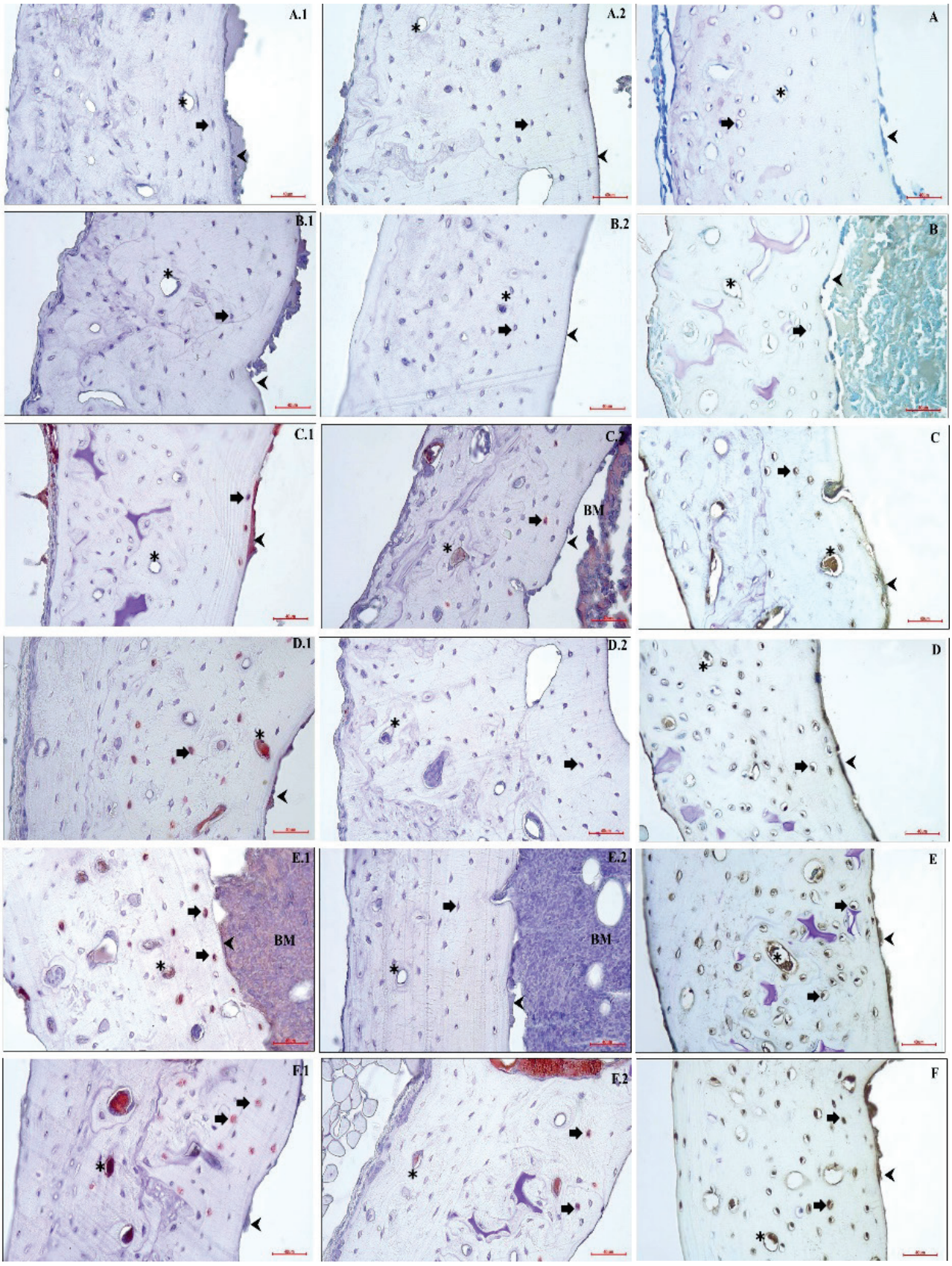

Fig. 5. Caspase 3 and 9, and Tunel staining images of tibia diaphyseal compact bone: (**A**) Caspase 3 (1) and Caspase 9 immunostain with Mayer's Hematoxylin floor paint (2), Control group: Group 1 (A1, A2, (**A**), Exposed groups; Group 2 (B1, B2, **B**), Group 3 (C1, C2, **C**), Group 4 (D1, D2, **D**), Group 5 (E1, E2, **E**), Group 6 (F1, F2, **F**). ➤: Osteoblast, ➡: Osteocyte, ✱: Haversian canals. x400) Bar = 40 µm. (**B**) Tunel staining images with Methyl green floor stain. (➤, and ➡): Tunel positive cells, ✱: Haversian canals. x400), Bar = 40 µm.

RANKL expression and increased OPG expression [4,8]. However, when osteoclasts from OVX rats were treated with a pulsed EMF, RANK expression showed no significant changes [24]. When OVX and hindlimb hanging rats were exposed to the pulsed EMF, neither RANK nor RANKL expression was changed [27,28]. Therefore, the EMF may not affect RANK but may increase the expression of OPG. Briefly, there is still controversy about the effects of EMF on RANKL expression, which may be related to different parameters and exposure time. Further studies are required to investigate the effects and mechanisms of EMF on the RANK/RANKL/OPG pathway.

In this study, we examined the effects and differences in bone formation between different EMF exposures and the control group to investigate the effect of exposure to 2.45 GHz MW radiation on pre/postnatal development. Additionally, the study was conducted only in male rats to rule out the possibility that EMF effects differ with gender. We observed functional and morphological changes in the bone after 10 and 15 V/m EMF exposure in rats exposed to MW radiation.

Discussion of RANK, RANKL, and OPG values

RANK, RANKL, and OPG are a series of cytokines related to the TNF family responsible for controlling bone formation and resorption. These cytokines are crucial for bone formation and maintenance of bone mass. Inflammatory cytokines regulate osteoclastogenesis and bone resorption by simulating RANKL production [29]. In our study, when the mean values of sRANKL were compared with the control group, it was observed that there was a statistically significant increase in the G5 and G6 groups. Increasing the RANKL value ensures osteoclast precursors' survival by participating in osteoclast differentiation. In a study by Lacey *et al*., advanced osteoporosis was observed with increased RANKL levels in genetically modified mice [30]. Fata *et al*. and Kong *et al*. reported that osteoclasts were destroyed and osteopetrosis developed in mice without RANKL [31,32]. Severe bone loss and hypercalcemia were reported in a study in mice treated with recombinant RANKL. At the same time, the OPG is a potent bone-protective agent, and RANKL is a pre-resorptive factor. In conclusion, *in vitro* experiments also support *in vivo* data [33-36]. Several studies in the literature examine the effects of an EMF on RANKL. Although studies have shown that low-frequency EMF improves the healing of bone fractures and increases bone mineral content [7,37], therapeutic EMF doses for osteoporosis have only been observed when pulsed at low doses of 15-72 Hz [38]. Long-term exposure to high doses of EMFs has also been reported to cause osteoporosis. Zhou *et al.* found that PEMF decreased RANKL expression and increased OPG expression by suppressing osteoclastogenesis through the OPG/RANK/RANKL signalling pathway [5]. However, in our current study, contrary to PEMFs, it can be concluded that RANKL levels were significantly higher than those in the control group, especially at 10 and 15 V/m EMF exposure, potentially showing activator effects through modulation of osteoclastogenesis. Osteoprotegerin (OPG) secreted by osteoblasts is a soluble “decoy receptor” for RANKL that inhibits the maturation of osteoclasts by blocking the activity of the RANKL/RANK signalling pathway [30]. In our study, when the OPG levels were compared with the control group, it was found that there was a statistically significant increase in the G5 and G6 groups. Zhou *et al.* reported that 8 Hz and 3.8 mT PEMF caused higher expression of the OPG in the lumbar, femur, and tibia while suppressing RANKL expression and preventing ovariectomy-induced bone loss [5]. However, Chen *et al.* observed no effect of PEMFs on RANK expression in osteoclast-like cells in ovariectomized rats [24]. In our study, the fact that high-frequency EMF application did not affect RANK values in growing rats supports these studies. Studies have shown that PEMFs can also significantly increase OPG and decrease the activation of IL-1beta-induced NF-kB p65 subunit [39]. The increase in OPG in the tibia of growing rats because of applying 10 and 15 V/m EMF at 2.45 GHz microwave frequency in both our study and SEMFs supports this study. Schwartz *et al.* showed that 15 Hz PEMF treatment increased the production of osteoblast OPG [40]. In another study, Shankar *et al.* found that it stimulated bone resorption through an effect on the osteoblast, restoring the response of osteoclasts to different cations [41]. These data suggest that EMFs can inhibit osteoclast proliferation and differentiation, and the effects on the balance between osteoblast and osteoclast by inducing apoptosis need further investigation. sRANKL and OPG expression was observed in many malignant and benign tumor cells [42-44]. Therefore, the sRANKL/OPG ratio has gained importance for bone pathologies. Essentially, any change in the sRANKL/OPG ratio leads to either excessive osteogenesis or excessive bone resorption, thereby affecting the rate of bone remodelling in the

sRANKL/OPG balance [29,45]. sRANKL/OPG balance is impaired in favor of sRANKL in osteolytic pathologies [46-48]. In these cases, high levels of OPG begin to be released to balance the sRANKL concentration in the tumor. The use of the sRANKL/OPG ratio as a prognostic biological factor in non-malignant pathologies such as osteoporosis, ankylosing spondylitis, rheumatoid arthritis, benign bone tumors, prosthetic osteolysis, and bone fractures is being investigated [49,50]. The increase in bone formation may occur due to an increase in OPG levels, also explained as a decrease in the sRANKL/OPG ratio. In contrast, pathological bone destruction occurs if the OPG level, also known as an increase in the sRANKL/OPG ratio, decreases and the sRANKL level increases [51]. In our study, when sRANKL/OPG levels were compared with those in the control group, it was found that there was a statistically significant decrease in the G5 and G6 groups. In other words, it may be thought that applying 10 and 15 V/m EMF increases bone formation by causing the OPG level to increase and the sRANKL level to decrease in the growing rat' tibia. This increase in bone formation increases osteoblasts, suggesting that it may be due to increased OPG expression. This is unsurprising since this study was applied to growing rats in the postnatal period. This situation shows us that the rats applied EMF have not yet entered the puberty period and have not completed the bone development period. Additionally, our findings are supported by histological examinations.

Discussion of histological data

Osteoclasts are giant multinucleated cells that can lyse calcified tissues derived from hematopoietic progenitor cells of the myelomonocytic lineage, which share a common precursor with macrophages. It has been expressed by osteoblasts, osteocytes and stromal cells. Postnatal bone remodelling is a dynamic process of balancing osteoclast-mediated bone resorption and osteoblast-mediated bone formation [52]. In our study, according to the results obtained from the histological data, it was determined that while there was a statistical increase in the osteoclasts of male rats in the postnatal period, there was a decrease in the number of osteoblasts. Bone homeostasis depends on the balanced activities between bone formation by osteoblasts and bone resorption by osteoclasts. The imbalance of bone formation and resorption causes various bone diseases. This imbalance, observed in our study because of an increase in osteoclasts and a decrease in osteoblasts, suggests that applying 10 and 15 V/m electric fields activates osteoclastogenesis by increasing the RANK/RANKL interaction.

When the effects of EMF on bone formation were examined, it was reported that they suppressed osteoclastic activity and increased osteoblastic activity [53]. Studies also show that it has no effect on bone [54]. Siddiqui and Partridge reviewed the role of cytokines in osteoclast development and found that interleukins-1 (IL-1), IL-6, and tumor necrosis factor (TNF) stimulate osteoclast development, whereas IL-4 and IL-18 inhibit osteoclast development [55]. Chang *et al.* examined the effect of EMFs on osteoclast formation in bone marrow cells from ovariectomized rats and found that osteoclast genesis could be inhibited by 7.5 Hz PEMF stimulation [8]. Bone and muscle tissue development were adversely affected due to prenatal exposure to 1800 MHz EMF [9]. Therefore, the effects of EMF on bone are still controversial. The imbalance between osteoblast and osteoclast in our study suggests that it may be due to bone diseases, the dose applied, and the fact that the rats are in the developmental period.

Bone homeostasis is regulated by osteoblasts, osteoclasts and osteocytes. Previous studies reported that radiation caused suppression of osteoblasts and osteocytes [56], and increased osteoclast differentiation [57]. In our study, the decrease in the number of osteoblasts and osteoclasts starting from G5 group and the irregular change in the number of osteoclasts caused the negative decrease of the radiation in the cells, and the increase in the expression of Caspase 3 and Caspase 9 starting from the G3 group showed us that osteoblasts and osteoclasts were negatively affected starting from 10 and 15 V/m EMF. It shows that it begins to be affected and triggers apoptosis in bone. Apoptosis is an important process that controls the physiological balance between cell replication and death. Apoptosis can be triggered by a wide variety of stimuli, disrupting cell cycle progression. Caspase 3 and 9 are the groups involved in the intrinsic mitochondrial pathway in apoptosis [58]. In our study, the highest caspase 3 and caspase 9 expression was observed in subjected to MW irradiation, especially in the G5 and G6 groups, suggesting that the radiation affected osteoblasts and osteocytes at increasing degrees from the intrinsic pathway to the apoptotic pathway, and thus may cause bone formation deterioration, bone loss and perhaps myelosuppression.

Apoptosis is a complex signal transformation

involving complex signal transformation and damage to cellular proteins and DNA [58]. In parallel with our Caspase findings, an increase in the number of Tunel-positive cells was observed in our groups exposed to radiation. The initiation of Tunel-positive cells, especially in the G3 group, from the 1.9 V/m electric field supported our previous studies, suggesting that this intensity is the threshold value that causes apoptosis to result in DNA damage in bone cells. As a result, there is no study in the literature to show the relationship between the EMF exposures of 2.45 MW radiation at different doses in the postnatal period on the RANK/RANKL/OPG system. Our study is the first in this area to examine the relationship between the RANK/RANKL/OPG systems and histological findings in the pre/postnatal period. In addition, our article is the first to propose a thermal and non-thermal effect level on the bone.

Conclusions

In the present study, the effects of 2.45 GHz MW radiation on the bone of healthy rat tibia exposed to different doses of EMF during the prenatal and postnatal period were investigated using biochemical methods such as RANK, RANKL, OPG, and histopathological methods such as Tunel and immunohistochemical straining. Our findings showed that 2.45 GHz low-level MW radiation at 10 V/m (the peak SAR 10g value 14.4 mW/kg) and 15 V/m (the peak SAR 10g value 33.8 mW/kg) could cause changes in the bone. To our knowledge, our study seems to be the first investigation in literature focusing on effects on the bone of 2.45 GHz low-level MW radiation at different EMF values. Additionally, this research is the first article to determine the level of thermal and non-thermal effects on bone.

Conflict of Interest

There is no conflict of interest.

Acknowledgements

We thank the Ondokuz Mayis University, Faculty of Engineering, Department of Electrical and Electronics Engineering.

References

1. Guidelines for Limiting Exposure to Electromagnetic Fields (100 kHz to 300 GHz). Health Phys 2020;118:483-524. https://doi.org/10.1097/HP.0000000000001210
2. Prucha J, Skopalik J, Socha V, Hanáková L, Knopfová L, Hána K. Two Types of High Inductive Electromagnetic Stimulation and Their Different Effects on Endothelial Cells. Physiol Res 2019;68:611-622. https://doi.org/10.33549/physiolres.933998
3. Misek J, Veternik M, Tonhajzerova I, Jakusova V, Janousek L, Jakus J. Radiofrequency Electromagnetic Field Affects Heart Rate Variability in Rabbits. Physiol Res 2020;69:633-643. https://doi.org/10.33549/physiolres.934425
4. Zhou J, Chen S, Guo H, Xia L, Liu H, Qin Y, He C. Pulsed electromagnetic field stimulates osteoprotegerin and reduces RANKL expression in ovariectomized rats. Rheumatol Int 2013;33:1135-1141. https://doi.org/10.1007/s00296-012-2499-9
5. Zhou J, Liao Y, Xie H, Liao Y, Zeng Y, Li N, Sun G, Wu Q, Zhou G. Effects of combined treatment with ibandronate and pulsed electromagnetic field on ovariectomy-induced osteoporosis in rats. Bioelectromagnetics 2017;38:31-40. https://doi.org/10.1002/bem.22012
6. Gürgül S, Erdal N, Yilmaz SN, Yıldız A, Ankaralı H. Deterioration of bone quality by long-term magnetic field with extremely low frequency in rats. Bone 2008;42:74-80. https://doi.org/10.1016/j.bone.2007.08.040
7. Chang K, Chang WH. Pulsed electromagnetic fields prevent osteoporosis in an ovariectomized female rat model: a prostaglandin E2-associated process. Bioelectromagnetics 2003;24:189-198. https://doi.org/10.1002/bem.10078
8. Chang K, Chang WH, Huang S, Shih C. Pulsed electromagnetic fields stimulation affects osteoclast formation by modulation of osteoprotegerin, RANK ligand and macrophage colony-stimulating factor. J Orthop Res 2005;23:1308-1314. https://doi.org/10.1016/j.orthres.2005.03.012.1100230611
9. Erkut A, Tumkaya L, Balik MS, Kalkan Y, Guvercin Y, Yilmaz A, Yuce S, Cure E, Sehitoglu I. The effect of prenatal exposure to 1800 MHz electromagnetic field on calcineurin and bone development in rats. Acta Cir Bras 2016;31:74-83. https://doi.org/10.1590/S0102-865020160020000001

10. Yasuda H. Discovery of the RANKL/RANK/OPG system. J Bone Miner Metab 2021;39:2-11. https://doi.org/10.1007/s00774-020-01175-1
11. Soysa NS, Alles N. Osteoclast function and bone-resorbing activity: An overview. Biochem Biophys Res Commun 2016;476:115-120. https://doi.org/10.1016/j.bbrc.2016.05.019
12. Manolagas SC, Parfitt AM. What old means to bone. Trends Endocrinol Metab 2010;21:369-374. https://doi.org/10.1016/j.tem.2010.01.010
13. Dallas SL, Prideaux M, Bonewald LF. The osteocyte: an endocrine cell ... and more. Endocr Rev 2013;34:658-690. https://doi.org/10.1210/er.2012-1026
14. Zimmerman SM, Heard-Lipsmeyer ME, Dimori M, Thostenson JD, Mannene EM, O'Brien CA, Morello R. Loss of RANKL in osteocytes dramatically increases cancellous bone mass in the osteogenesis imperfecta mouse (oim). Bone Rep 2018;9:61-73. https://doi.org/10.1016/j.bonr.2018.06.008
15. Wada T, Nakashima T, Hiroshi N, Penninger JM. RANKL-RANK signaling in osteoclastogenesis and bone disease. Trends Mol Med 2006;12:17-25. https://doi.org/10.1016/j.molmed.2005.11.007
16. Suda T, Takahashi N, Udagawa N, Jimi E, Gillespie MT, Martin TJ. Modulation of osteoclast differentiation and function by the new members of the tumor necrosis factor receptor and ligand families. Endocr Rev 1999;20:345-357. https://doi.org/10.1210/edrv.20.3.0367
17. Yasuda H, Shima N, Nakagawa N, Yamaguchi K, Kinosaki M, Mochizuki S, Tomoyasu A, Yano K, Goto M, Murakami A, Tsuda E, Morinaga T, Higashio K, Udagawa N, Takahashi N, Suda T. Osteoclast differentiation factor is a ligand for osteoprotegerin/osteoclastogenesis-inhibitory factor and is identical to TRANCE/RANKL. Proc Natl Acad Sci U S A 1998;95:3597-3602. https://doi.org/10.1073/pnas.95.7.3597
18. Simonet WS, Lacey DL, Dunstan CR, Kelley M, Chang MS, Lüthy R, Nguyen HQ, ET AL. Osteoprotegerin: a novel secreted protein involved in the regulation of bone density. Cell 1997;89:309-319. https://doi.org/10.1016/S0092-8674(00)80209-3
19. Hofbauer LC, Schoppet M. Clinical implications of the osteoprotegerin/RANKL/RANK system for bone and vascular diseases. JAMA 2004;292:490-495. https://doi.org/10.1001/jama.292.4.490
20. Elabd SK, Sabry I, Hassan WB, Nour H, Zaky K. Possible neuroendocrine role for oxytocin in bone remodeling. Endocr Regul 2007;41:131-141.
21. Hsu H, Lacey DL, Dunstan CR, Solovyev I, Colombero A, Timms E, Tan H-Lin, ET AL. Tumor necrosis factor receptor family member RANK mediates osteoclast differentiation and activation induced by osteoprotegerin ligand. Proc Natl Acad Sci U S A 1999;96:3540-3545. https://doi.org/10.1073/pnas.96.7.3540
22. Boyce BF and Xing L. Biology of RANK, RANKL, and osteoprotegerin. Arthritis Res Ther 2007;9(Suppl 1):S1. https://doi.org/10.1186/ar2165
23. Kearns AE, Khosla S, Kostenuik PJ. Receptor activator of nuclear factor kappaB ligand and osteoprotegerin regulation of bone remodeling in health and disease. Endocr Rev 2008;29:155-192. https://doi.org/10.1210/er.2007-0014
24. Chen J, He HC, Xia QJ, Huang LQ, Hu YJ, He CQ. Effects of pulsed electromagnetic fields on the mRNA expression of RANK and CAII in ovariectomized rat osteoclast-like cell. Connect Tissue Res 2010;51:1-7. https://doi.org/10.3109/03008200902855917
25. Ando K, Mori K, Rédini F, Heymann D. RANKL/RANK/OPG: key therapeutic target in bone oncology. Curr Drug Discov Technol 2008;5:263-268. https://doi.org/10.2174/157016308785739857
26. Pacheco R, Stock H. Effects of radiation on bone. Curr Osteoporos Rep 2013;11:299-304. https://doi.org/10.1007/s11914-013-0174-z
27. Jing D, Li F, Jiang M, Cai J, Wu Y, Xie K, Wu X, Tang C, Liu J, Guo W, Shen G, Luo E. Pulsed electromagnetic fields improve bone microstructure and strength in ovariectomized rats through a Wnt/Lrp5/β-catenin signaling-associated mechanism. PLoS One 2013;8:e79377. https://doi.org/10.1371/journal.pone.0079377
28. Jing D, Cai J, Wu Y, Shen G, Li F, Xu Q, Xie K, Tang C, Liu J, Guo W, Wu X, Jiang M, Luo E. Pulsed electromagnetic fields partially preserve bone mass, microarchitecture, and strength by promoting bone formation in hindlimb-suspended rats. J Bone Miner Res 2014;29:2250-2261. https://doi.org/10.1002/jbmr.2260
29. Kwan Tat S, Padrines M, Théoleyre S, Heymann D, Fortun Y. IL-6, RANKL, TNF-alpha/IL-1: interrelations in bone resorption pathophysiology. Cytokine Growth Factor Rev 2004;15:49-60. https://doi.org/10.1016/j.cytogfr.2003.10.005

30. Lacey DL, Timms E, Tan HL, Kelley MJ, Dunstan CR, Burgess T, Elliott R, Colombero A, Elliott G, Scully S, Hsu H, Sullivan J, Hawkins N, Davy E, Capparelli C, Eli A, Qian YX, Kaufman S, Sarosi I, Shalhoub V, Senaldi G, Guo J, Delaney J, Boyle WJ. Osteoprotegerin ligand is a cytokine that regulates osteoclast differentiation and activation. Cell 1998;93:165-176. https://doi.org/10.1016/S0092-8674(00)81569-X
31. Fata JE, Kong YY, Li J, Sasaki T, Irie-Sasaki J, Moorehead RA, Elliott R, Scully S, Voura EB, Lacey DL, Boyle WJ, Khokha R, Penninger JM. The osteoclast differentiation factor osteoprotegerin-ligand is essential for mammary gland development. Cell 2000;103:41-50. https://doi.org/10.1016/S0092-8674(00)00103-3
32. Kong YY, Feige U, Sarosi I, Bolon B, Tafuri A, Morony S, Capparelli C, ET AL. Activated T cells regulate bone loss and joint destruction in adjuvant arthritis through osteoprotegerin ligand. Nature 1999;402:304-309. https://doi.org/10.1038/46303
33. Anderson DM, Maraskovsky E, Billingsley WL, Dougall WC, Tometsko ME, Roux ER, Teepe MC, DuBose RF, Cosman D, Galibert L. A homologue of the TNF receptor and its ligand enhance T-cell growth and dendritic-cell function. Nature 1997;390:175-179. https://doi.org/10.1038/36593
34. Burgess TL, Qian Y, Kaufman S, Ring BD, Van G, Capparelli C, Kelley M, Hsu H, Boyle WJ, Dunstan CR, Hu S, Lacey DL. The ligand for osteoprotegerin (OPGL) directly activates mature osteoclasts. J Cell Biol 1999;145:527-538. https://doi.org/10.1083/jcb.145.3.527
35. Darnay BG, Haridas V, Ni J, Moore PA, Aggarwal BB. Characterization of the intracellular domain of receptor activator of NF-kappaB (RANK). Interaction with tumor necrosis factor receptor-associated factors and activation of NF-kappab and c-Jun N-terminal kinase. J Biol Chem 1998;273:20551-20555. https://doi.org/10.1074/jbc.273.32.20551
36. Min H, Morony S, Sarosi I, Dunstan CR, Capparelli C, Scully S, Van G, Kaufman S, Kostenuik PJ, Lacey DL, Boyle WJ, Simonet WS. Osteoprotegerin reverses osteoporosis by inhibiting endosteal osteoclasts and prevents vascular calcification by blocking a process resembling osteoclastogenesis. J Exp Med 2000;192:463-474. https://doi.org/10.1084/jem.192.4.463
37. Bilotta TW, Zati A, Gnudi S, Figus E, Giardino R, Fini M, Pratelli L, Mongiorgi R. Electromagnetic fields in the treatment of postmenopausal osteoporosis: an experimental study conducted by densitometric, dry ash weight and metabolic analysis of bone tissue. Chir Organi Mov 1994;79:309-313.
38. Atay T, Aksoy BA, Aydogan NH, Baydar ML, Yildiz M, Ozdemir R. Effect of electromagnetic field induced by radio frequency waves at 900 to 1800 MHz on bone mineral density of iliac bone wings. J Craniofac Surg 2009;20:1556-1560. https://doi.org/10.1097/SCS.0b013e3181b78559
39. Vincenzi F, Targa M, Corciulo C, Gessi S, Merighi S, Setti S, Cadossi R, Goldring MB, Borea PA, Varani K. Pulsed electromagnetic fields increased the anti-inflammatory effect of A_2A and A_3 adenosine receptors in human T/C-28a2 chondrocytes and hFOB 1.19 osteoblasts. PLoS One 2013;8:e65561. https://doi.org/10.1371/journal.pone.0065561
40. Schwartz Z, Fisher M, Lohmann CH, Simon BJ, Boyan BD. Osteoprotegerin (OPG) production by cells in the osteoblast lineage is regulated by pulsed electromagnetic fields in cultures grown on calcium phosphate substrates. Ann Biomed Eng 2009;37:437-444. https://doi.org/10.1007/s10439-008-9628-3
41. Shankar VS, Simon BJ, Bax CM, Pazianas M, Moonga BS, Adebanjo OA, Zaidi M. Effects of electromagnetic stimulation on the functional responsiveness of isolated rat osteoclasts. J Cell Physiol 1998;176:537-544. https://doi.org/10.1002/(SICI)1097-4652(199809)176:3<537::AID-JCP10>3.0.CO;2-X
42. Blair JM, Zhou H, Seibel MJ, Dunstan CR. Mechanisms of disease: roles of OPG, RANKL and RANK in the pathophysiology of skeletal metastasis. Nat Clin Pract Oncol 2006;3:41-49. https://doi.org/10.1038/ncponc0381
43. Dougall WC, Chaisson M. The RANK/RANKL/OPG triad in cancer-induced bone diseases. Cancer Metastasis Rev 2006;25:541-549. https://doi.org/10.1007/s10555-006-9021-3
44. Holen I, Shipman CM. Role of osteoprotegerin (OPG) in cancer. Clin Sci (Lond) 2006;110:279-291. https://doi.org/10.1042/CS20050175
45. Theoleyre S, Wittrant Y, Tat SK, Fortun Y, Redini F, Heymann D. The molecular triad OPG/RANK/RANKL: involvement in the orchestration of pathophysiological bone remodeling. Cytokine Growth Factor Rev 2004;15:457-475. https://doi.org/10.1016/j.cytogfr.2004.06.004

46. Giuliani N, Bataille R, Mancini C, Lazzaretti M, Barille S. Myeloma cells induce imbalance in the osteoprotegerin/osteoprotegerin ligand system in the human bone marrow environment. Blood 2001;98:3527-3533. https://doi.org/10.1182/blood.V98.13.3527
47. Grimaud E, Soubigou L, Couillaud S, Coipeau P, Moreau A, Passuti N, Gouin F, Redini F, Heymann D. Receptor activator of nuclear factor kappaB ligand (RANKL)/osteoprotegerin (OPG) ratio is increased in severe osteolysis. Am J Pathol 2003;163:2021-2031. https://doi.org/10.1016/S0002-9440(10)63560-2
48. Voskaridou E, Terpos E. Osteoprotegerin to soluble receptor activator of nuclear factor kappa-B ligand ratio is reduced in patients with thalassaemia-related osteoporosis who receive vitamin D3. Eur J Haematol 2005;74:359-361. https://doi.org/10.1111/j.1600-0609.2004.00395.x
49. Granchi D, Pellacani A, Spina M, Cenni E, Savarino LM, Baldini N, Giunti A. Serum levels of osteoprotegerin and receptor activator of nuclear factor-kappaB ligand as markers of periprosthetic osteolysis. J Bone Joint Surg Am 2006;88:1501-1509. https://doi.org/10.2106/JBJS.E.01038
50. Veigl D, Niederlová J, Kryštůfková O. Periprosthetic osteolysis and its association with RANKL expression. Physiol Res 2007;56:455-462. https://doi.org/10.33549/physiolres.930997
51. Bostanci N, Ilgenli T, Emingil G, Afacan B, Han B, Töz H, Berdeli A, Atilla G, McKay IJ, Hughes FJ, Belibasakis GN. Differential expression of receptor activator of nuclear factor-kappaB ligand and osteoprotegerin mRNA in periodontal diseases. J Periodontal Res 2007;42:287-293. https://doi.org/10.1111/j.1600-0765.2006.00946.x
52. Bique AM, Kaivosoja E, Mikkonen M, Paulasto-Kröckel M. Choice of osteoblast model critical for studying the effects of electromagnetic stimulation on osteogenesis in vitro. Electromagn Biol Med 2016;35:353-364. https://doi.org/10.3109/15368378.2016.1138124
53. Chang Y, Hu CC, Wu YY, Ueng SWN, Chang CH, Chen MF. Ibudilast Mitigates Delayed Bone Healing Caused by Lipopolysaccharide by Altering Osteoblast and Osteoclast Activity. Int J Mol Sci 2021;22:1169. https://doi.org/10.3390/ijms22031169
54. Sert C, Mustafa D, Düz MZ, Akşen F, Kaya A. The preventive effect on bone loss of 50-Hz, 1-mT electromagnetic field in ovariectomized rats. J Bone Miner Metab 2002;20:345-349. https://doi.org/10.1007/s007740200050
55. Siddiqui JA, Partridge NC. Physiological Bone Remodeling: Systemic Regulation and Growth Factor Involvement. Physiology (Bethesda) 2016;31:233-245. https://doi.org/10.1152/physiol.00061.2014
56. Sakurai T, Sawada Y, Yoshimoto M, Kawai M, Miyakoshi J. Radiation-induced reduction of osteoblast differentiation in C2C12 cells. J Radiat Res 2007;48:515-521. https://doi.org/10.1269/jrr.07012
57. Willey JS, Lloyd SA, Robbins ME, Bourland JD, Smith-Sielicki H, Bowman LC, Norrdin RW, Bateman TA. Early increase in osteoclast number in mice after whole-body irradiation with 2 Gy X rays. Radiat Res 2008;170:388-392. https://doi.org/10.1667/RR1388.1
58. Wu G, Chen X, Peng J, Cai Q, Ye J, Xu H, Zheng C, Li X, Ye H, Liu X. Millimeter wave treatment induces apoptosis via activation of the mitochondrial-dependent pathway in human osteosarcoma cells. Int J Oncol 2012;40:1543-1552. https://doi.org/10.3892/ijo.2012.1330